PAPER 4

Radar-based forest biomass estimation

In: International Journal of Remote Sensing 1994.
Vol. 15, No. 14, pp. 2797–2808.

INT. J. REMOTE SENSING, 1994, VOL. 15, NO. 14, 2797–2808

Radar-based forest biomass estimation

Y. RAUSTE, T. HÄME

Technical Research Centre of Finland, Space Technology,
Metallimiehenkuja 10, FIN-02150 Espoo, Finland

J. PULLIAINEN, K. HEISKA and M. HALLIKAINEN

Helsinki University of Technology, Laboratory of Space Technology,
Otakaari 5 A, SF-02150 Espoo, Finland

Abstract. The potential of radar-based tree biomass estimation has been studied using polarimetric SAR data from the Freiburg test site of the MAESTRO 1 Campaign and scatterometer data from a test site in Finland. Using the Freiburg SAR data and polarizaiton synthesis, the most suitable polarization combination was obtained. In *P* band, the maximum correlations, which were found near the linear *HV* polarization, were up to 0·75.

In the Finnish test site, a strong negative correlation (correlation coefficient −0·65) existed between the pine biomass and *X-VV* backscatter. When the combination of *X* and *C* bands (measured by the HUTSCAT scatterometer) was used, a correlation coefficient of 0·81 was obtained.

1. Introduction

The biomass of forests affects the circulation of carbon in the biosphere. Tropical forests are a carbon source, while many temperate and boreal forests are a carbon sink. It has been estimated that the annual build-up of carbon in European forests alone is 50 million tons (Kauppi *et al.* 1992). Forests also produce raw material for a variety of industrial activities. There are large areas in the boreal forest zone where the amount and distribution of forest biomass is poorly known.

Mapping of forest biomass using radar has been studied (e.g., Sader 1987, Hussin *et al.* 1991, Le Toan *et al.* 1991) in recent years. Sader (1987) studied the relationship between *L*-band polarimetric SAR data and the biomass of two pine species (longleaf pine, *Pinus palustris* Mill. and slash pine, *Pinus elliotti* Englem.). The terrain elevation in the study site varied from 3 to 15 m above sea level. Sader found a correlation coefficient of 0·76 between the *L-HV* digital number and biomass in a set of nine stands. The *HH* and *VV* polarizations did not have significant correlation with biomass. The green weight biomass ranged from 25 to 230 t ha^{-1}.

Hussin *et al.* (1991) studied the estimation of slash pine biomass using *L*-band polarimetric SAR data. The age of the stands in the study varied between 4 and 31 years. In a dataset of 35 stands, a coefficient of determination (r^2) 0·97 was obtained with *HV* polarized SAR data. The Box–Cox power transformation was applied to the biomass data before they were used in regression analyses.

Le Toan *et al.* (1991) studied the relationship between multi-band polarimetric SAR data and stem biomass. The study site consisted of homogeneous stands of

0143–1161/94 $10.00 © 1994 Taylor & Francis Ltd

maritime pine (*Pinus pinaster* Ait.). The forest had been planted on flat soil. The age varied from 0 to 42 years and the stem biomass from 0 to $105\,\mathrm{t\,ha^{-1}}$. High correlations between the stem biomass and the relative backscattering coefficient were obtained for *VH*, *HH*, and *VV* polarizations in *P* band (r^2 values of 0·95, 0·90 and 0·88, respectively). The relationship between the stem biomass and the relative backscattering coefficient was linear throughout the whole biomass range (0–$105\,\mathrm{t\,ha^{-1}}$) and no saturation was observed.

Owing to differences in the species composition or forest management practices, the test sites of these studies are not representative of large natural forests in the Eurasian part of the boreal forest zone.

The study described in this article was carried out in the context of the MAESTRO 1 Campaign, organized jointly by the Joint Research Centre of the European Communities and the European Space Agency.

The possibilities for the use of radar in tree biomass estimation are studied using polarimetric SAR data from the Freiburg test site. Scatterometer data from a test site in Ruotsinkylä in Finland are studied to supplement and enlarge the findings of the study based on SAR data.

Processing and analysis of the SAR data has been carried out mainly by the Instrument laboratory of the Technical Research Centre of Finland. Measurement, processing and analysis of the scatterometer data have been carried out by the Laboratory of Space Technology of the Helsinki University of Technology.

2. Study sites and measurement data

2.1. *Freiburg test site and SAR data*

Data from the Freiburg test site of the MAESTRO 1 Campaign was used in the study. The test site (centre at 48°02′25″ N, 8°22′01″ E) is located near the town of Villingen-Schwenningen in south-west Germany. Terrain elevation at the test site varies between 750 and 970 metres above sea level. The area is dominated by temperate coniferous forests. Norway spruce (*Picea abies* Karst.) covers 1370 ha, Scots pine (*Pinus sylvestris* L.) 280 ha and Silver fir (*Abies alba* Mill.) approximately 200 ha of the 1920 ha study area. Deciduous trees are distributed sparsely in the area. Stem volume in the study area varies between 0 and $830\,\mathrm{m^3\,ha^{-1}}$. Age varies from 0 to 180 years.

The ground data from the test site included a forest map at a scale of 1:10 000 and standwise forest inventory data for 230 forest stands. The map and forest inventory data were based on a field inventory in 1980. A trial, based on the average relationship between stand age and stem volume, was made to update the stem volume information. Ground observations in June 1991 revealed that this updating was very unreliable. The original ground data were used in analyses.

Direct measurements of the biomass of the forest were not available. Stem volume was used to represent the forest biomass. According to other studies (Häme *et al.* 1992), the stem volume (in $\mathrm{m^3\,ha^{-1}}$) could be approximately converted into dry biomass of trees (in $\mathrm{kg\,ha^{-1}}$) by multiplying the stem volume by 600. In the absence of more accurate data on the biomass in the test site, this simple transformation has been used in this study where standwise data are analysed. For example, a stem volume of $800\,\mathrm{m^3\,ha^{-1}}$ corresponds approximately to a dry biomass of $480\,000\,\mathrm{kg\,ha^{-1}}$ ($48\,\mathrm{kg\,m^2}$).

Two scenes of the Freiburg SAR data (Churchill *et al.* 1990) were used: scenes 1105 and 1107. The SAR data (fully polarimetric images in *C*, *L* and *P* bands) were acquired using the AIRSAR sensor (Held *et al.* 1988). The incidence angle in the study site ranged from 35° to 55° in scene 1105 and from 48° to 55° in scene 1107. The SAR data were acquired on 18 August 1989 with no rain on the preceeding two days.

Figure 1 shows the processing steps applied to the data before the data were used in the analyses (Rauste 1992). The topography normalization utilizes the equation:

$$R_{\mathrm{norm}} = \frac{R_{\mathrm{orig}}\sqrt{\tan(\theta_{\mathrm{r}})}}{\sqrt{\tan(\theta_{\mathrm{nom}})}} \tag{1}$$

where R_{norm} = normalized radar return (amplitude), R_{orig} = original radar return (amplitude), θ_{r} = incidence angle in range direction, and θ_{nom} = nominal incidence angle. The angle θ_{r} was computed for each pixel using a digital elevation model. Standwise averaged Stokes matrix data were used in the search for the best band polarization combination for tree biomass mapping.

2.2. *Ruotsinkylä test site and scatterometer data*

The helicopter-borne scatterometer measurements were performed in the Ruotsinkylä research area of the Finnish Forest Research Institute. The test site is located near Helsinki (centre at 60°21′23″ N, 25°00′48″ E). The total length of test lines for helicopter-borne scatterometer measurements was 4 km. The dominant tree species in the test lines were Scots pine and Norway spruce. The test lines were divided into 20 m by 20 m sample plots for the data analysis. The measured forest characteristics of each sample plot included:

(*a*) average tree height,
(*b*) mean tree stem diameter at a height of 1·3 m,
(*c*) mean tree stem diameter at a height of 6 m and
(*d*) density (number of tree stems per hectare).

Detailed information on the ground truth database is given in Hyyppä and Hyyppä (1992). The basal area ($m^3\,ha^{-1}$) was calculated on the basis of stem diameter measurements at a height of 1·3 m. The stem volume was calculated on the basis of stem diameter measurements at 1·3 m and 6 m and tree height measurements.

In this analysis, a total of 150 sample plots were used; 96 of these were pine dominated and the rest were spruce dominated sample plots. The tree height for the sample plots varies from 1 to 27 m, and the stem volume per hectare varies from 0 to 370 $m^3\,ha^{-1}$.

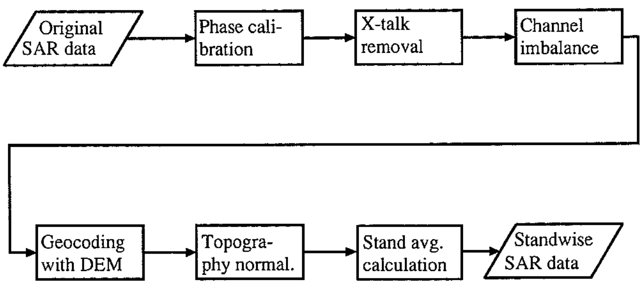

Figure 1. Preprocessing steps applied to SAR data.

The scatterometer data were acquired with the HUTSCAT instrument under winter conditions in December 1991. The ground surface temperature was -5° C, and the thickness of snow-cover was between 0 and 5 cm. The HUTSCAT scatterometer is an 8-channel helicopter-borne non-imaging ranging scatterometer operating at *C* and *X* bands (5 and 10 GHz) at *HH*, *VV*, *VH* and *HV* polarizations (Hyyppä and Hallikainen 1991). The scatterometer measures the backscattered power versus range along the flight line (in 1-m intervals). The backscattering coefficient of the target is calculated from the radar return versus range profiles. A video camera is used for positioning the radar measurements in relation to the corresponding forest sample plots. The application of the HUTSCAT instrument for forest measurements is described in Hallikainen *et al.* (1990).

The HUTSCAT instrument is both internally and externally calibrated. The internal calibration data are recorded for each measurement sequence. The absolute level of internal calibration is determined by external calibration, performed with Luneberg lenses and active radar calibrators.

The HUTSCAT scatterometer is an FM-CW radar that measures the backscattering properties of a target versus range in real time. This is accomplished by performing a 512-point FFT to the intermediate frequency of the radar. The radar cross-section of a target (in dB) is calculated by summing the power received from the target for different intermediate frequencies (ranges), and by using internal calibration. This result is directly comparable with the SAR measurement. The backscattering coefficient (σ^0, expressed in dB) can be determined by dividing the radar cross-sections of different ranges with the illuminated areas corresponding to different ranges.

3. Analysis methods

In the analysis of the polarimetric SAR data, a systematic search was employed to find the best band polarization combination for tree biomass mapping. Starting with the standwise average Stokes matrix data and the standwise stem volume data, the following operations were carried out for each possible polarization combination (combination of transmit orientation, transmit ellipticity, receive orientation and receive ellipticity):

(*a*) the received power was calculated for each stand using polarization synthesis (van Zyl *et al.* 1987),
(*b*) the linear correlation coefficient between the stem volume and the radar amplitude (square root of the received power) was calculated.

The polarization combination that gave the highest correlation with stem volume was considered to be the best for biomass mapping. The space of all possible polarization combinations was processed in a grid with a step of 10°. The polarization optimization described above was carried out separately for each radar band.

Linear regression analysis was used, in the analysis of both SAR and scatterometer data, to estimate the accuracy with which the tree stem volume can be estimated from SAR data. In the analysis of the polarimetric SAR data, the ground data was split into two subsets: one for determination of the linear regression model (the learning set) and another for testing the model. Correlation coefficients were computed for the whole ground dataset. When the correlation coefficient exceeded

0·4, the estimation error E for the linear model was computed:

$$E=\sqrt{\frac{\Sigma(V_{est}-V_{real})^2}{n-1}} \qquad (2)$$

where V_{est} is the stem volume estimate given by the model, V_{real} is the stem volume in the ground data and n is the number of observations in the testing set.

For the analysis of the HUTSCAT data, the average backscattering coefficient of each forest sample plot was calculated. The average value was taken from 20 scatterometer measurements for a sample plot.

4. Estimation of tree biomass from SAR data

The polarization optimization procedure decribed earlier was applied over the whole 4-dimensional space of receive and transmit orientation and ellipticity. The highest stem-volume–radar correlations were found in P band and close to the original HV polarization. As the highest correlations were found close to the original polarizations (HH, HV and VV) the following concentrates on the original polarizations. Table 1 shows the correlations obtained for each band. The last line of the table was obtained with data from scene 1107 (larger incidence angle) and the other lines with data from scene 1105. The L-band correlations were studied using two datasets: (1) the whole dataset with stem volume 0–830m^3 ha^{-1} and (2) the subset with stem volume 0–170 m^3 ha^{-1}. The L-band amplitude seems to reach its saturation level somewhere close to 150 m^3 ha^{-1}. Thus, the correlation between L-band amplitude and stem volume is higher in the stem volume range 0–170 m^3 ha^{-1} than in the whole range of 0–830 m^3 ha^{-1}. The size of the 0–170 m^3 ha^{-1} ground dataset (72 stands) did not allow splitting into the learning and testing sets.

Figure 2 shows the radar HV amplitude as a function of stem volume for C, L and P bands. The dashed lines in the P-band diagram show the confidence limits of the regression model at 1 per cent confidence. As observed in other studies (e.g. Kasischke *et al.* 1991, Dobson *et al.* 1991) the backscatter saturates at a biomass level that depends on the wavelength. The relationship between the stem volume and radar amplitude is linear in P-HV. In L-HV, the radar amplitude first increases with

Table 1. SAR backscatter (amplitude) *vs.* stem volume.

Band-polarization	Stem volume range (m^3 ha^{-1})	Correlation coefficient	Estimation error (m^3 ha^{-1})	
			Learning	Testing
C-HV	0–830	−0·37	—	—
C-HH	0–830	−0·33	—	—
C-VV	0–830	−0·06	—	—
L-HV	8–830	−0·19	—	—
L-HV	0–170	0·47	41·7	—
L-HH	0–170	0·50	40·9	—
L-VV	0–170	0·43	42·5	—
P-HV	0–830	0·73	135·6	141·7
P-HH	0–830	0·31	—	—
P-VV	0–830	0·21	—	—
P-HV (1107)	0–830	0·65	145·9	168·2

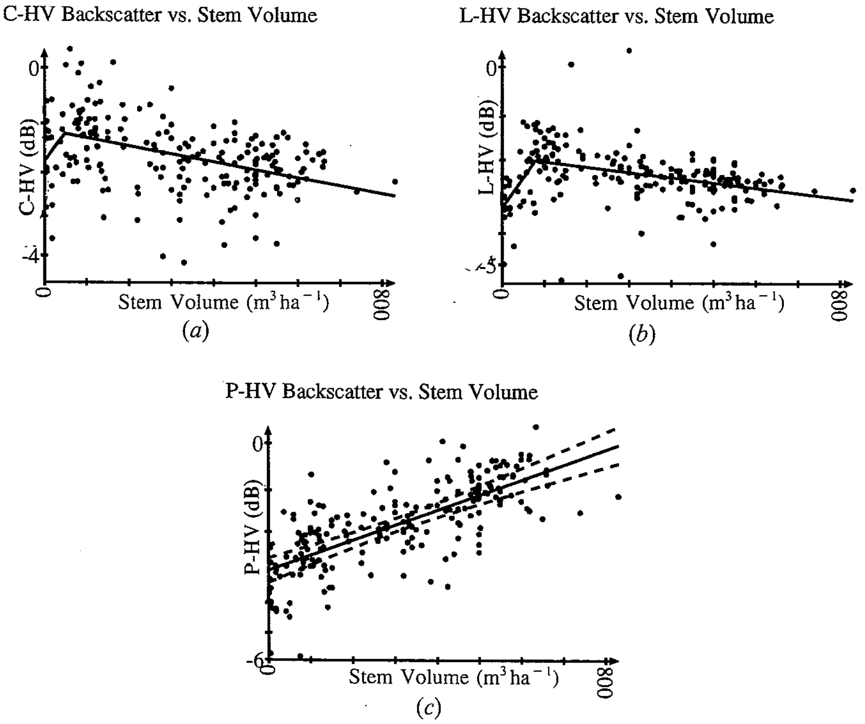

Figure 2. Radar amplitude as a function of stem volume in the Freiburg test site. (*a*) *C*-band; (*b*) *L*-band; (*c*) *P*-band.

increasing stem volume content. After a stem volume of about $120\,\mathrm{m^3\,ha^{-1}}$, the radar amplitude decreases with increasing stem volume. A stem volume of $120\,\mathrm{m^3\,ha^{-1}}$ corresponds to a dry biomass of about $7\,\mathrm{kg\,m^{-2}}$. In *C* band, the radar amplitude reaches its saturation level at about $60\,\mathrm{m^{-3}\,ha^{-1}}$ (about $3{\cdot}5\,\mathrm{kg\,m^{-2}}$ dry biomass).

Figure 3 shows the correlation coefficient between the stem volume and the radar amplitude as a function of the polarization combination. The possible polarization combinations form a 4-dimensional space (receive orientation, receive ellipticity, transmit orientation and transmit ellipticity). Only two 2-dimensional subsets of the 4-dimensional space are shown in figure 3. In the copolarized diagram, the receive orientation equals the transmit orientation and the receive ellipticity equals the transmit ellipticity. In the cross-polarized diagram, the receive orientation is at right angles to the transmit orientation and the receive ellipticity equals the negative transmit ellipticity. In *P* band, the highest correlations form a very narrow peak around the linear *HV* polarization. In *L* band, the correlations are lower but less dependent on the polarization combination. In the *L*-band diagram, only those stands where the stem volume was less than $170\,\mathrm{m^3\,ha^{-1}}$ were included.

As no absolute calibration was carried out on the SAR, the coefficients of the linear regression models between the SAR amplitude and stem volume are not reported here. The models were of the form:

$$V_{\mathrm{est}} = ax + b, \tag{3}$$

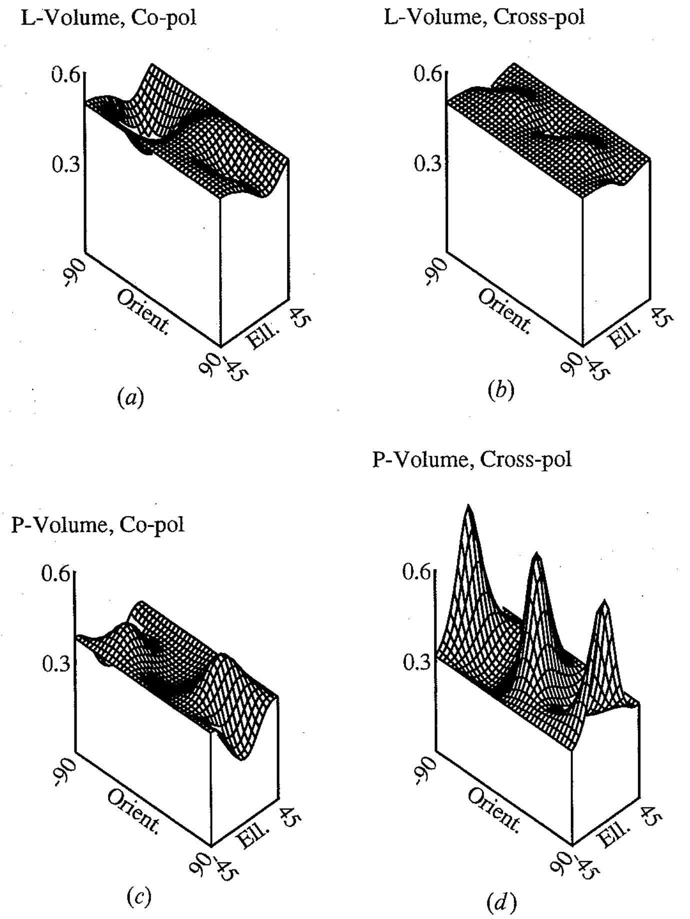

Figure 3. Correlation coefficient between the radar amplitude and stem volume as a function of polarization combination (Freiburg test site). (*a*) *L*-band, co-pol.; (*b*) *L*-band, cross-pol.; (*c*) *P*-band, co-pol.; (*d*) *P*-band, cross-pol.

where a and b are the coefficients of the model and x is the radar amplitude. Figure 4 shows the stem volume estimate using *P-HV* data.

5. Estimation of tree biomass from scatterometer data

Tables 2 and 3 show the correlation coefficients between forest characteristics and different scatterometer channels. The results imply that the response of the *C*-band channels to the changes in forest characteristics is negligible. The channel showing the highest correlation between the stem volume and the backscattering coefficient is *X*-band *VV* polarization (figure 5). The backscattering coefficient decreases with increasing stem volume, except for stem volume values smaller than $50\,m^3\,ha^{-1}$.

Figure 6 demonstrates the feasibility of a multi-channel instrument for stem volume estimation. The results shown in figure 6 were obtained by a multiple linear regression model for the stem volume (only pine sample plots were employed). The

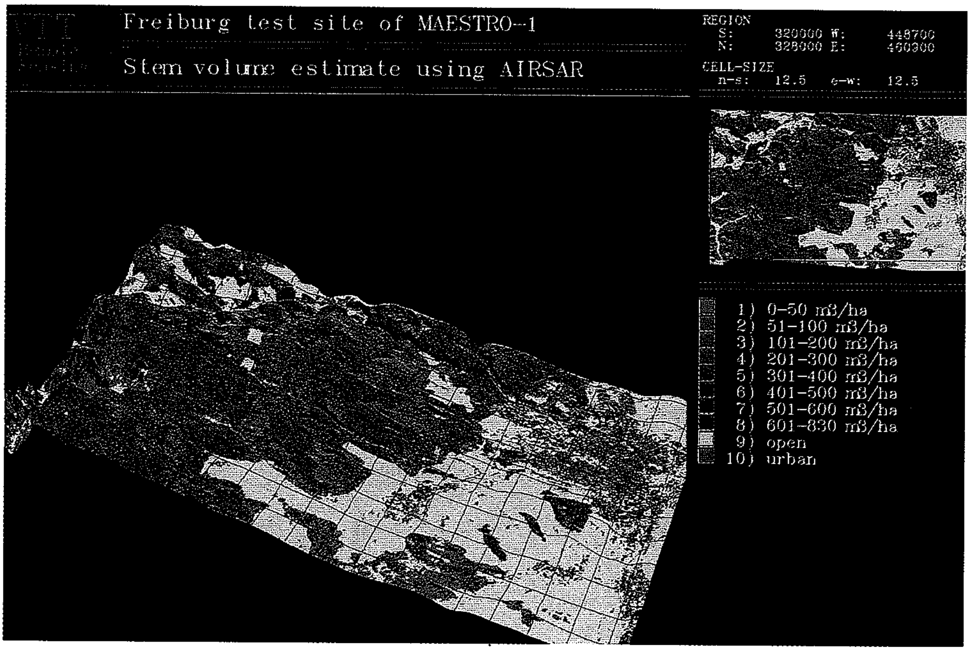

Figure 4. SAR-based (*P-HV*) stem volume estimate of the Freiburg test site.

correlation coefficient is 0·75 ($r^2=0{\cdot}56$). The same equation gives a correlation coefficient of 0·81 ($r^2=0{\cdot}66$), when two neighbouring sample plots are averaged in both the ground truth data and the scatterometer data.

6. Discussion

The highest correlations between tree biomass and backscatter found in the Freiburg test site were similar but slightly lower than those found by Hussin *et al.* (1991) or Le Toan *et al.* (1991). Several factors may have contributed to the lower correlations. The topography of the Freiburg test site was more pronouncced than that in the French test site studied by Le Toan *et al.* (1991). Residual topographic effects (after topographic normalization) have contributed to the lower correlation in the Freiburg test site. The topography could also explain the lower *HH* correlation, which according to Beaudoin *et al.* (1992) depends strongly on local slope. The stands in the Freiburg test site were mainly mixed stands and not single-

Table 2. Correlation coefficients (*r*) for the whole Ruotsinkylä dataset (pine- and spruce-dominated sample plots); 150 sample plots.

	C-HH	*C-HV*	*C-VH*	*C-VV*	*X-HH*	*X-HV*	*X-VH*	*X-VV*
Stem volume	−0·08	0·02	0·00	−0·02	−0·37	−0·34	−0·35	−0·57
Basal area	−0·02	0·07	−0·03	−0·03	−0·20	−0·23	−0·22	−0·40
Mean diameter	−0·03	0·03	−0·01	−0·04	−0·30	−0·35	−0·32	−0·49
Density	0·07	0·12	−0·14	−0·01	0·18	0·34	0·33	−0·25
Average height	−0·17	−0·20	−0·12	−0·10	−0·38	−0·40	−0·39	−0·46

Table 3. Correlation coefficients (r) for pine-dominated sample plots in the Ruotsinkylä test site; 96 sample plots.

	C-HH	*C-HV*	*C-VH*	*C-VV*	*X-HH*	*X-HV*	*X-VH*	*X-VV*
Stem volume	−0·03	0·08	0·11	0·08	−0·44	−0·59	−0·55	−0·65
Basal area	0·15	0·30	0·22	0·01	−0·12	−0·24	−0·22	−0·29
Mean diameter	0·12	0·12	0·13	0·03	−0·27	−0·49	−0·40	−0·49
Density	0·03	0·09	0·09	−0·05	0·19	0·36	−0·34	0·33
Average height	−0·07	−0·20	0·02	0·03	0·36	−0·45	−0·40	−0·42

species stands as in Hussin *et al.* (1991) or Le Toan *et al.* (1991). Also, the range of biomass in the Freiburg test site was larger than that in Hussin *et al.* (1991) or Le Toan *et al.* (1991). The relatively low accuracy (due to a 9-year interval between the forest inventory and the SAR image acquisition) may also have contributed to the lower correlation.

In the analysis of the Freiburg SAR data, a positive correlation between *P-HV* backscatter and tree biomass was found in the biomass range of 0–50 $\mathrm{kg\,m^{-2}}$. In *L*-band, there was a positive correlation at 0–7 $\mathrm{kg\,m^{-2}}$ after which the backscatter decreased slowly with increasing biomass. In *C* band, there was a weak positive correlation in the range 0–3·5 $\mathrm{kg\,m^{-2}}$ after which the backscatter decreased more rapidly than in *L* band.

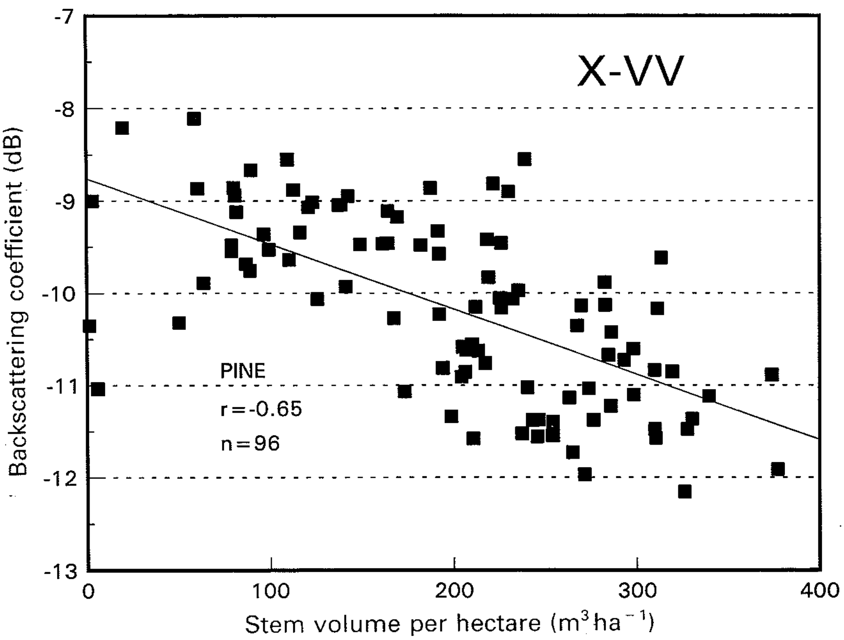

Figure 5. Backscattering coefficient as a function of stem volume per hectare for *X*-band *VV* polarization (Ruotsinkylä test site). Excluding data points with a stem volume below 50 $\mathrm{m^3\,ha^{-1}}$ increases the correlation coefficient (r) from 0·65 to 0·71. Measurements were made on 17 December 1991.

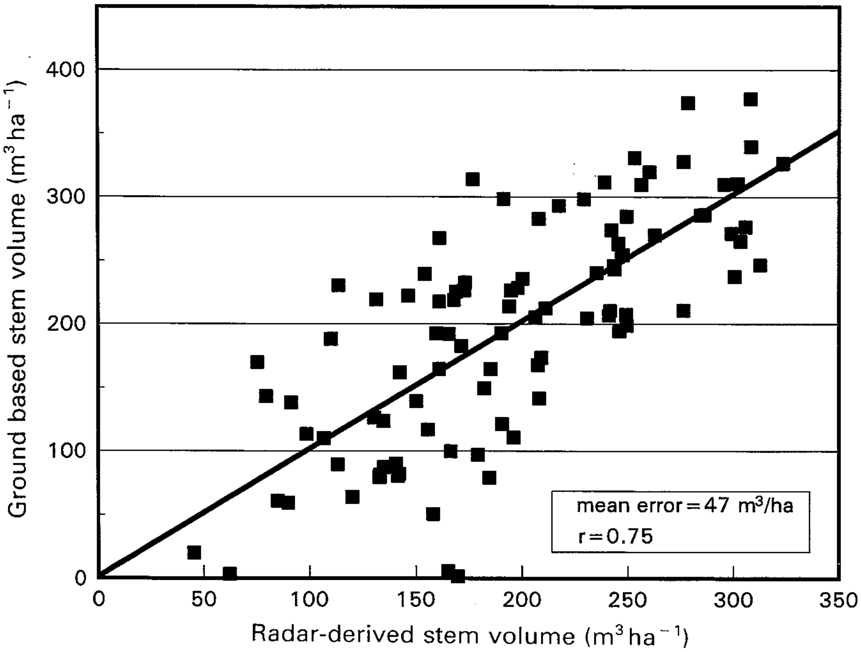

Figure 6. Ground-based volume versus radar-based estimate from multiple linear regression equation employing X-VV, and C- and X-band cross-polarized channels (Ruotsinkylä-test site). Pine forest 17 December 1991. The formula used to calculate the radar-derived stem volume was:

$$V(\mathrm{m^3\,ha^{-1}}) = 657 - 637\frac{\sigma^0_{C\text{-}VH}}{\sigma^0_{X\text{-}HV}} - 165\frac{\sigma^0_{C\text{-}HV}}{\sigma^0_{X\text{-}VH}} - 28\,\sigma^0_{X\text{-}VV}$$

In the analysis of the scatterometer data, the C-band backscatter was found to be almost independent of biomass. In X band, there was a positive correlation at 0–25 $\mathrm{kg\,m^{-2}}$ after which the backscatter decreased rapidly with increasing biomass. The decrease is most likely to be due to increased attenuation of the ground–trunk backscattering and increased attenuation of the direct backscattering from the ground. Figure 7 shows a schematic representation of the radar backscatter at P, L, C and X bands.

The C band of the SAR aboard the ERS-1 satellite does not seem to be very promising for tree biomass estimation. Two types of radar sysems could be used in tree biomass mapping: (1) a system with a long wavelength and cross-polarization (P-HV) or (2) a system with a short wavelength (X-VV). In the first case, the correlation between backscatter and biomass is positive. In the second case, the correlation is negative. In areas where the biomass level is less than about 10 $\mathrm{kg\,m^{-2}}$, forest biomass could also be mapped with SAR in L band, which is present aboard an existing satellite (JERS-1).

Acknowledgments

The authors would like to thank the Finnish Technology Development Centre TEKES and the Central Association of Finnish Forest Industries (Suomen Metsäteollisuuden Keskusliitto) for funding the study.

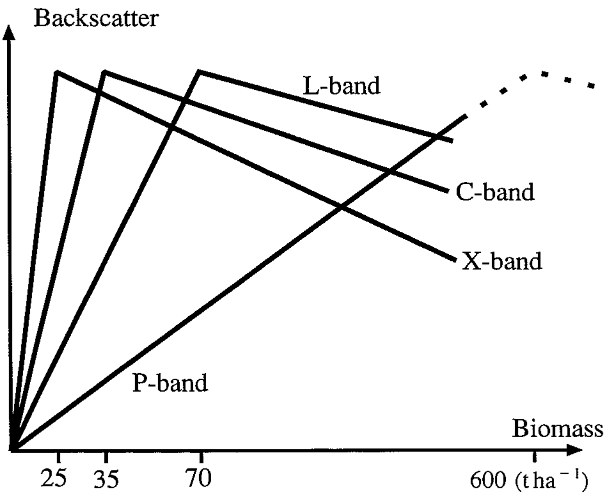

Figure 7. Schematic representation of the radar backscatter as a function of tree biomass at *P*, *L*, *C* and *X* band.

References

BEAUDOIN, A., LE TOAN, T., HSU, C., HAN, H., KONG, J., and SHIN, J., 1992, Simulation of forest backscatter as a function of forest and ground parameters. *Proceedings of IGARSS '92, 22-29 May, Houston, Texas* (Piscataway, New Jersey, USA: Institute of Electrical and Electronics Engineers), pp. 1212-1214.

CHURCHILL P., ATTEMA, E., BAKER, J., BLYTH, K., BIRD, P., BOUMAN, S., UENK, D., VISSERS, M., DROESEN, W., GUYON, D., RIOM, J., HOEKMAN, D., VAN LEEUWEN, H., VAN DER SANDEN, J., KOBRIK, M., SHEN, Y., CARANADE, R., KUNTZ, S., LE TOAN, T., BEAUDOIN, A., MITCHELL, P., WIELOGORSKI, A., and WOODING, M., 1990, MAESTRO 1 airborne synthetic aperture radar (SAR) campaign 1989, Data report, JRC/Ispra and ESA, June 1990 (Ispra, Italy: Joint Research Centre, Institute for Remote Sensing Applications), 198 pp.

DOBSON, M., MCDONALD, K., and SHARIK, T., 1991, Relating the temporal change observed by AIRSAR to surface and canopy properties of mixed conifer and hardwood forests of northern Michigan. *Proceedings of the Third Airborne Synthetic Aperture Radar (AIRSAR) Workshop, 23-24 May*, JPL Publication, 91-30, pp. 34-43.

HALLIKAINEN, M., TARES, T., HYYPPÄ, J., SOMERSALO, E., AHOLA, P., TOIKKA, M., and PULLIAINEN, J., 1990, Helicopter-borne measurements of radar backscatter from forests, *International Journal of Remote Sensing*, **11**, 1179-1191.

HÄME, T., SALLI, A., and LAHTI, K., 1992, Estimation of carbon storage in boreal forests using remote sensing data, Pilot study. In M. Kanninen, and P. Anttila, (editors), *The Finnish research programme on climate change, Progress report* (Helsinki, Finland: Publications of the Academy of Finland 3/92), pp. 250-255.

HELD, D., BROWN, W., FREEMAN, A., KLEIN, J., ZEBKER, H., SATO, T., MILLER, T., NGUYEN, Q., and LOU, Y., 1988, The NASA/JPL multifrequency, multipolarization airborne SAR system, *Proceedings of IGARSS'88 September, Edinburgh, Scotland* (Paris: European Space Agency), pp. 345-350.

HUSSIN, Y., REICH, R., and HOFFER, R., 1991., Estimating slash pine biomass using radar backscatter, *I.E.E.E. Transactions on Geoscience and Remote Sensing*, **29**, 427-431.

HYYPPÄ, J., and HYPPÄ, H., 1992, A database and software tools for developing algorithms in forest inventory, Report 8, Laboratory of Space Technology, Helsinki University of Technology, 40 pp.

HYYPPÄ, J., and HALLIKAINEN, M., 1991, Development of a helicopter-borne 8-channel ranging scatterometer, Report 4, Laboratory of Space Technology, Helsinki University of Technology, 24 pp.

LE TOAN, T., BEAUDOIN, A., RIOM, J., and GUYON, D., 1991, Relating forest parameters to SAR data, *Proceedings of IGARSS'91, Helsinki University of Technology, Espoo, Finland, 3-6 June*, Vol. II (New York, USA: Institute of Electrical and Electronics Engineers), pp. 689-692.

KASISCHKE, E., BOURGEAU-CHAVEZ, L., CHRISTENSEN, N., and DOBSON, C., 1991, The relationship between aboveground biomass and radar backscatter as observed on airborne SAR imagery, *Proceeding of the Third Airborne Synthetic Aperture Radar (AIRSAR) Workshop, 23-24 May*, JPL Publication 91-30 (New York, U.S.A.: Institute of Electrical and Electronics Engineers), pp. 11-21.

KAUPPI, P., MIELIKÄINEN, K., and KUUSELA, K., 1992, Biomass and carbon budget of European forests, 1971 to 1990, *Science*, **256**, 70-74.

RAUSTE, Y., 1992, Geometric/radiometric preprocessing of SAR scattering matrix data, *Proceedings of the final workshop of the MAESTRO 1 and AGRISCATT Campaigns, Noordwijk, The Netherlands, 6-7 February* (Paris: European Space Agency), pp. 113-116.

SADER, S., 1987, Forest biomass, canopy structure, and species composition relationships with multipolarization *L*-band synthetic aperture radar data, *Photogrammetric Engineering and Remote Sensing*, **53**, 193-202.

VAN ZYL, J., ZEBKER, H., and ELACHI, C., 1987, Imaging radar polarization signatures: Theory and observation, *Radio Science*, **22**, 529-543.